

Attosecond photon sources: the first decade and beyond [Invited]

Zenghu Chang^{1,2,*} and P. Corkum³

¹*Florida Attosecond Science and Technology Laboratory, Department of Physics and CREOL, University of Central Florida, Orlando, Florida 32816, USA*

²*J. R. Macdonald Laboratory, Department of Physics, Kansas State University, Manhattan, Kansas 66506, USA*

³*Joint Attosecond Science Laboratory, University of Ottawa and National Research Council of Canada, 100 Sussex Drive, Ottawa, Ontario K1A 0R6, Canada*

*Corresponding author: zechang@mail.ucf.edu

Received June 24, 2010; revised August 22, 2010; accepted August 22, 2010;
posted August 23, 2010 (Doc. ID 130620); published October 1, 2010

Attosecond optics is a young branch of ultrafast laser science. In this short review, we introduce some of the important advancements and latest developments in generating and characterizing single isolated attosecond XUV/X-ray pulses. © 2010 Optical Society of America
OCIS codes: 320.0320, 140.7240.

1. INTRODUCTION

The demonstration of lasers, 50 years ago, enabled the development and exploitation of perturbative nonlinear optics. Among the many consequences of the partnership between lasers and nonlinear optics, have been the development of mode-locking and the emergence of ultrashort pulse (even single-cycle) lasers. Over the decades, short pulse technology was continually improved until we reached the single-cycle limit.

Femtosecond lasers, in turn, have enabled the development and exploitation of nonperturbative nonlinear optics. Femtosecond pulses are so valuable because only the fastest (and therefore the simplest) processes have a chance to grow. Among the many consequences of the partnership between femtosecond lasers and nonperturbative optics has been the emergence of attosecond pulses. As we will see below, for attosecond technology, ionizing atoms or molecules are the preferred nonlinear medium.

From the prospective of attosecond science, the high order of the light-atom interaction allows us to work below the period of the light-cycle. It is as though we had much shorter wavelength radiation. The ability to work beneath the laser period is a general characteristic of high-order nonlinearity, widely appreciated in plasma physics. Using the re-collision [1] method that we will describe below, researchers will continue to shorten pulses from the current limit of 100 as to a few attoseconds. But recollision is just the first of a series of nonlinear methods that will generate attosecond pulses. We can almost certainly look forward to high-energy zeptosecond pulses in the relatively near future.

In general, any process that has the response time to create an attosecond pulse also has a response time to measure the pulse or to measure attosecond processes that we may wish to study. There are a number of specific procedures, but all use ionizing atoms as the nonlinear

medium. Generically, this procedure is referred to as the attosecond streak camera. Named in 1997 [2] before the first attosecond pulses were generated, it will be described below.

With this technology, three classes of attosecond (or attosecond-like) measurements have been reported. First attosecond pulses can be used much like femtosecond pulses. That is, they can be produced (as we describe below) then transported to a medium where they interact with a material with an unknown response to be measured. An impressive example of this approach to attosecond measurement is determination of the emission dynamics of photoelectrons from Tungsten [3]. Second, the generating medium for attosecond pulses is also the probed medium. In this case the generating medium is excited before the attosecond pulse is to be produced. Producing the attosecond pulse serves as a probe; the change in the emitted spectrum as a function of pump-probe time delay reports on the process. An example is the complete characterization of the dissociation dynamics of molecular Bromine [4]. Finally, an attosecond pulse is not required at all as long as the underlying strong field physics that lead to attosecond pulses is used. An example is the attosecond strobing of a strong driven two-level system dynamics [5] or time-resolving the position hydrogen atoms in hydrogen bearing molecules [6] during the first few femtoseconds following tunnel ionization.

We have emphasized that high-order nonlinear interactions allow us to “sub-divide” the laser period and thereby make attosecond pulses and attosecond measurements. It must be also possible to operate below the laser wavelength—*space as well as time*. In fact, extreme nonlinear optics opens the potential to directly image atomic-scale matter [7–12]. Imaging methods have been developed hand-in-hand with attosecond pulse generation. Although the body of this paper emphasizes pulse generation and measurement, the reader should keep in mind

the opportunity of measuring and manipulating small spatial dimensions as they read the following sections. We will briefly discuss imaging in the conclusion of the paper.

2. PRINCIPLE OF ATTOSECOND PULSE GENERATION AND CHARACTERIZATION

Attosecond XUV pulses are generated by interacting intense femtosecond lasers with noble gases. The center wavelength of the most commonly used Ti:sapphire laser is 800 nm, which corresponds to an optical period of $T_0 = 2.67$ fs. The attosecond pulse generation process can be understood by the semiclassical three-step model developed in 1993, which is depicted in Fig. 1 [1,13]. According to this model, the whole process of generating an attosecond pulse takes place in one laser cycle. The process repeats every half of a cycle when the laser is linearly polarized and contains many cycles, which leads to an attosecond pulse train. In the frequency domain, the interference of attosecond pulses in the train produces discrete peaks separated by two-laser photon energy called high-order harmonics. As a comparison, the spectrum of an isolated attosecond pulse is an XUV continuum.

A. Semiclassical Model

Here we focus on what happens in one laser cycle.

1. First Step: Releasing of Attosecond Electron Bunches

When the electric field strength of the laser is comparable to that of the atomic Coulomb force, an attosecond electron wave packet can be released from the atom during a fraction of a laser cycle by tunneling through the potential barrier formed by the superposition of the Coulomb field and the laser field. The strength of the Coulomb field of noble gases is close to one atomic unit. One atomic unit of intensity is 3.55×10^{16} W/cm². The laser intensity used in attosecond pulse generation experiments is on the order of 10^{14} to 10^{15} W/cm², which is orders of magnitude higher than what was used in nonlinear optics studies with solid materials ($< 10^{13}$ W/cm²).

In the tunneling ionization regime, the probability of releasing an electron can be estimated by simple equations. The most commonly used one is the Ammosov-Delone-Krainov (ADK) rate [14]. When a laser pulse interacts with an atom, the ionization from each cycle adds up. An isolated attosecond pulse is generated within one laser cycle of the whole pulse, the ground-state population of the atom should not be fully depleted by ionization before the cycle where the attosecond pulse is generated.

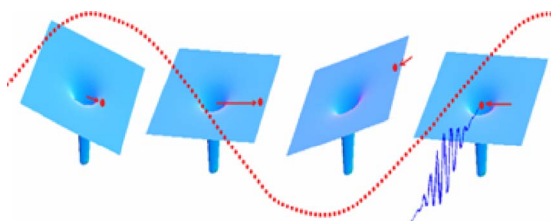


Fig. 1. (Color online) Semiclassical model of attosecond pulse generation. Adapted from P. B. Corkum and F. Krausz, Nat. Phys. 3, 381 (2007).

The requirement puts a major constrain on the laser field for generating isolated pulses. For sufficiently higher laser intensity, the atom can be fully ionized just before the useful cycle. That value is defined as the saturation intensity I_S , which is 10^{14} to 10^{15} W/cm² for noble gases.

2. Second Step: Electron Acceleration

Once an electron tunnels out from the barrier, its motion is mostly controlled by the laser field which is much stronger than the Coulomb field when the distance of the electron to the nucleus is sufficiently large. The electron trajectory can be conveniently calculated by solving Newton's equation, which is a big advantage of the semiclassical model.

The solution reveals that only electrons released during a certain time period in a laser cycle can return to the parent ion to produce attosecond XUV photons. The initial velocity of the electron is almost zero. During the returning journey, the electron is accelerated by the laser field. For electrons in an attosecond wave packet, the returning kinetic energy varies with the returning time, which introduces a chirp to the attosecond electron pulse. The maximum energy gain is $3.17U_p$, where U_p is the ponderomotive energy, which is proportional to laser intensity I_0 and wavelength square λ^2 . The round trip time for an electron to gain the maximum energy is about half a laser cycle. The electron that returns earlier than the one with maximum kinetic energy takes a "short trajectory", whereas the one that returns later goes through a "long trajectory." The short-trajectory electron pulse is positively chirped, meaning the kinetic energy increases with the returning time.

In attosecond pulse generation experiments, the density of the noble gas target is $\sim 10^{18}$ /cm³. The size of the target is on the order of millimeters. It turns out that radiations from the short trajectory have lower beam divergence than that from the long trajectory. Thus they can be easily separated in the far field where photon emissions from all the target atoms are collected by a detector. In most applications, the short trajectory is used. Consequently, the attosecond photon pulses are positively chirped. The amount of chirp is $\sim 0.5T_0/3.17U_p \propto 1/I_0\lambda$, which suggests that the chirp can be reduced by either using high laser intensity or increasing the laser wavelength.

3. Third Step: Attosecond Photon Pulse Emission

An attosecond photon pulse is emitted when the attosecond electron wave packet returns to the parent ion. The photon energy is equal to the ionization potential plus the kinetic energy of the returning electron that makes the transition to the ground state. For electrons taking the short trajectory, their positive chirp is transferred to the photon pulses. The chirp needs to be removed to yield the transform-limited pulse. The duration of such pulses is limited by their frequency bandwidth. A transform-limited 25 as Gaussian pulse corresponds to a bandwidth of 75 eV FWHM.

The attosecond light pulse is generated from the electric dipole radiation. The photon emission rate is related to the dipole moment

$$\vec{r}(t) = \langle \Psi_g(\vec{r}, t) | \vec{r} | \Psi_c(\vec{r}, t) \rangle, \quad (1)$$

where $\Psi_g(\vec{r}, t)$ and $\Psi_c(\vec{r}, t)$ are the wave functions of the ground state of the target atom and continuum state, respectively. Above the ionization saturation intensity, the ground state is completely depleted, i.e., $\Psi_g(\vec{r}, t) = 0$. No isolated attosecond pulse can be generated. Therefore, in isolated attosecond pulse-generation experiments, the ionization caused by the laser field before the cycle where the desirable three-step process occurs should not fully deplete the ground-state population. The maximum kinetic energy of the returning electron and thus the highest photon energy, named cut-off energy, is determined by the saturation intensity.

For given atom and laser pulse parameters, the cut-off photon energy $\hbar\omega_c$ is limited by the depletion of the ground-state population in the cycles before the one where the isolated attosecond pulse is generated. Assuming the laser is linearly polarized and that we wish to generate an attosecond pulse during the cycle at the peak of the pulse, then [15]

$$\hbar\omega_c = I_P + \left[\frac{0.5I_P^{3.5}\lambda^2}{\ln\left(\frac{0.86I_P 3^{2n^* - 1} G_{lm} C_{n^* l^*}^2}{-\ln(1 - p_S)} \tau_p\right)} \right]^2, \quad (2)$$

where p_S is the ionization probability at the peak of the pulse that defines the saturation of the ionization of the ground-state population, which can be set to 0.98. The unit of $\hbar\omega_c$ and ionization potential I_P is eV. The unit of laser wavelength λ is μm . The laser pulse duration (FWHM) τ_p is in femtoseconds. The values of n^* , G_{lm} , and $C_{n^* l^*}^2$ are found in [14]. Equation (2) shows the explicit dependence of the cut-off photon energy and, thus, the attosecond bandwidth on the atomic and laser parameters.

Equation (2) indicates that one approach to increase the cut-off photon energy is to use long-wavelength driving lasers. This was first demonstrated in the XUV wavelength range in 2001 [16]. Figure 2(a) is the high-order

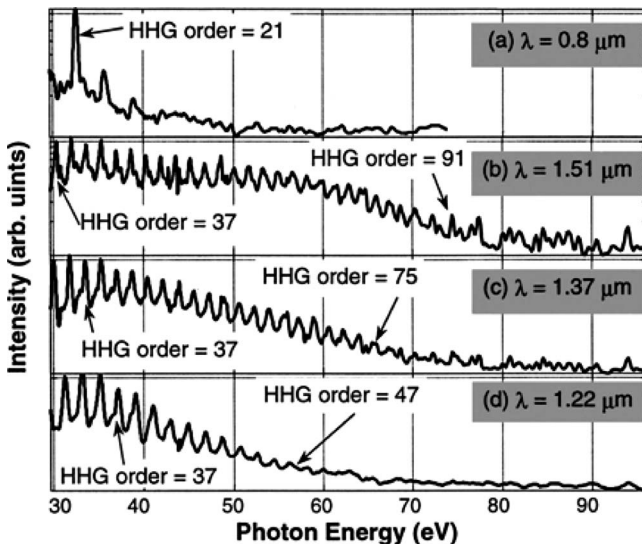


Fig. 2. Experimental demonstration of cut-off extension by increasing the driving laser wavelength. Adapted from B. Shan and Z. Chang, Phys. Rev. A 65, 011804(R) (2001).

harmonic spectrum from xenon atoms obtained with a 0.8 μm laser. Figures 2(b)–2(d) are the results produced by using an optical parametric amplifier (OPA) pumped by the 0.8 μm laser. The OPA was tuned at 1.51, 1.37, and 1.22 μm , respectively. Obviously, the cut-off was dramatically extended when the 1.51 μm OPA was used.

Equation (2) revealed that the cut-off photon energy depends on the cube of the ionization potential energy of the target atom. It was predicted that keV soft X-rays could be generated by interacting helium atoms (which has the largest I_P among neutral atoms) with lasers centered at 1.6 μm . Recently, phase-matched X-rays in the “water window” have been generated using mid-IR OPAs by several groups [17–19]. Using long-wavelength lasers may lead to coherent zeptosecond X-ray pulses in the future.

B. Strong Field Approximation

The semiclassical model is extremely intuitive. With this model one can calculate the chirp and cut-off photon energy of attosecond pulses. A quantum version of the three-step model was developed in 1994 [20], which allows us to find out the attosecond pulse shape and phase from a single atom. It is also useful for understanding the characterization of attosecond pulses.

1. For Attosecond Generation

The quantum model calculates the dipole moment in Eq. (1) based on the strong field approximation, which ignores the effects of excited states and assumes the continuum states are plane waves. As a result, the dipole moment can be calculated by an integral,

$$\vec{r}(t) = i \int_0^\infty d\tau \left(\frac{\pi}{\epsilon + i\frac{\tau}{2}} \right)^{3/2} a^*(t) \vec{d}^*[\vec{p}_S(t, \tau) - \vec{A}_L(t)] e^{iS(\vec{p}_S, t, \tau)} \vec{E}_L(t - \tau) \cdot \vec{d}[\vec{p}_S(t, \tau) - \vec{A}_L(t - \tau)] a(t - \tau) + c.c. \quad (3)$$

where $\vec{E}_L(t)$ is the driving laser field, which frees the electron from the ground state with population $|a(t - \tau)|^2$ through the dipole transition $\vec{E}_L(t - \tau) \cdot \vec{d}[\vec{p}_S(t, \tau) - \vec{A}_L(t - \tau)]$ at time $t - \tau$. The freed electron wave acquires a phase $S(\vec{p}_S, t, \tau)$ and then recombines with the ground state with a population of $|a(t)|^2$ through another dipole transition at time t . It explicitly shows the ground-state population cannot be completely depleted for generating attosecond pulses

The integral can be performed on a personal computer in seconds to minutes, which is much faster than solving the time-dependent Schrödinger equation numerically. The fast speed is important for simulating the attosecond pulse generation from a gas target, which needs the single atom response for millions of atoms.

2. For Attosecond Characterization

The strong field approximation also plays an important role in characterizing attosecond pulses. At the present time, it is difficult to perform autocorrelation of attosecond pulses based on the second or high-order nonlinear effects like what has been done for characterizing femtosecond laser pulses. This is because of the low attosecond pulse power as a result of poor conversion efficiency (typi-

cally 10^{-6}) from the driving laser to the XUV pulse. Instead, attosecond pulse characterization is based on cross-correlation with a femtosecond field oscillation that changes a full cycle in a few femtoseconds. The experiments are done by first converting the attosecond photon pulse into an attosecond electron pulse through photoelectric emission in atoms. An intense NIR laser field interacts with the freed electron, giving the electron a momentum kick [2,21]. By measuring the electron spectrum variation as a function of time delay between the NIR field and the attosecond pulse, one can deduce the attosecond pulse duration. The spectrogram is related to the amplitude of electron wave in the continuum with momentum \vec{v} at delay τ_d :

$$b(\vec{v}, \tau_d) = i \int_{-\infty}^{\infty} dt \vec{E}_X(t - \tau_d) \cdot \vec{d}[\vec{v}] + \vec{A}_L(t) e^{-i \int_t^{\infty} [(\vec{v} + \vec{A}_L(t'))^2/2 + I_P] dt'}, \quad (4)$$

where $\vec{E}_X(t)$ is the attosecond pulse to be characterized, $\vec{d}(\vec{v})$ is the dipole transition matrix element from the ground state to the continuum state. $\vec{A}_L(t)$ is the vector potential of the NIR laser. The expression was derived under the strong field approximation [22], which assumed that the continuum states are plane waves. The intensity of the NIR laser is 10^{12} to 10^{13} W/cm², which is intense enough to change the momentum of the electrons in the continuum states but does not ionize the bound state. Expression [4] is similar to that of the frequency resolved optical gating (FROG) technique for characterizing femtosecond lasers [23]. Consequently, the pulse retrieval algorithm developed for FROG can also be used to reconstruct attosecond pulses, which leads to the complete reconstruction of attosecond burst (CRAB) method [24].

The iterative phase retrieval algorithm used by CRAB assumes that the spectral bandwidth of the attosecond pulse is smaller than the center energy of the photoelectrons, which is named central momentum approximation. It limits the shortest attosecond pulse that can be characterized by CRAB. Very recently, it was discovered that $\int_{-\infty}^{\infty} d\tau_d |b(\vec{v}, \tau_d)|^2 e^{-i\omega\tau_d}$ consists of a series of peaks centered at $\omega = m\omega_L$, $m = 0, 1, 2, \dots$, where ω_L is the NIR frequency. When the laser intensity is low ($\sim 10^{11}$ W/cm²), the spectral phase of the attosecond pulse can be retrieved from the signals in the $\omega = \omega_L$ peak. This scheme, dubbed PROOF (phase retrieval by omega oscillator filtering), can be applied to extremely short attosecond pulses, since it does not require the central momentum approximation [25].

3. CARRIER-ENVELOPED PHASE-STABILIZED DRIVING LASERS

The required laser intensities 10^{14} to 10^{15} W/cm², for generating attosecond pulses, are obtained by focusing femtosecond millijoule (or higher) pulses to a spot less than 50 μm . The most commonly used driving lasers are based on chirped pulse amplification (CPA), where femtosecond pulses with a few nanojoules of energy from an oscillator are stretched to tens or hundreds of picoseconds before seeding multipass or regenerative amplifiers to

avoid damaging of the gain medium. The amplified pulses are compressed to tens of femtoseconds. Prism or grating pairs are commonly used to stretch and compress optical pulses. The laser pulses from CPA lasers can be further compressed down to pulses that contain only a few optical cycles. Single isolated attosecond pulses are generated in one laser cycle, thus the energy contained in other cycles cannot be converted to attosecond pulse energy. For achieving high conversion efficiency, the laser pulse duration should be as short as possible.

The attosecond pulse emission time is locked to the carrier wave oscillation, as the three-step model revealed. This makes the timing between the carrier wave and the envelope of the pulse important. The carrier-envelope (CE) phase of the driving laser needs to be locked for generating identical single isolated attosecond pulses from shot to shot. Very recently, it was demonstrated that attosecond XUV pulses with identical duration and contrast can be generated with arbitrary CE phase values using the generalized double optical gating to be discussed in Section 4. The CE phase only affects the intensity of the XUV pulses.

A. CE Phase in Grating-Based CPA Systems

The electric field of a linearly polarized transform-limited laser pulse can be expressed as

$$E(t) = E_A(t) \cos(\omega_0 t + \varphi_{CE}), \quad (5)$$

where $E_A(t)$ is the pulse envelope function and ω_0 is the carrier angular frequency. The CE phase φ_{CE} is defined as the offset between the peak of the pulse envelope and the nearest maximum of the field oscillation.

For the grating pairs used in the optical stretchers and compressors, it was shown that, in a double-pass configuration, if the spacing between the gratings is changed by an amount ΔG , the CE phase will have a shift [26]

$$\Delta\varphi_{CE} = 4\pi \frac{\Delta G}{d} \tan[\beta(\omega_0)], \quad (6)$$

where d is the grating constant, which is on the order of 1 μm . β is the diffraction angle. For typical setups, $\tan[\beta(\omega_0)] \approx 1$, thus a change of grating spacing on the order of sub-micrometer by vibration and thermal expansion can cause a large CE phase variation (on the order of π radians). Vibration management is extremely important for developing CE phase stabilized lasers.

B. CE Phase Stabilization

To deliver CE phase stabilized laser pulses on the gas target for generating isolated attosecond pulses, the shot-to-shot CE phase variation in the oscillator, CPA, and hollow-core fiber compressor must be eliminated.

1. Oscillator Phase Locking

The repetition rate of the femtosecond oscillator is on the order of 80 MHz. Instead of locking the CE phase of all pulses to the same value, the change rate of the CE phase, which is named the CE offset frequency f_0 , can be conveniently locked. f_0 is sensitive to the power of the pump laser on the gain medium, which can be locked to a fraction of the repetition rate by controlling the pump power with

an acousto-optic modulator (AOM). The locking scheme was demonstrated for frequency metrology in 2000 [27,28]. f_0 is also susceptible to the temperature of the gain medium. By adding a second feedback loop that controls the gain crystal temperature, the CE offset frequency can be locked for 19 hours [29], as shown in Fig. 3.

2. CPA Phase Stabilization by Controlling the Grating Separation

The CE phase of CPA lasers has been stabilized by feedback-controlling the separation of gratings in either stretchers or compressors [30,31]. The gratings are displaced by piezoelectric transducers. The feedback loop is separated from the one that stabilizes the CE offset frequency and thus does not interfere with the oscillator operation, which leads to long phase-locking time. The scheme has been developed to lock CE phase of CPA systems based on either multipass or regenerative designs.

The CE phase error signal is measured with f -to- $2f$ interferometers for the feedback control [32,33]. In the f -to- $2f$ setup, a few microjoules of pulse energy are focused to a sapphire plate to form a filamentation, which produces a white-light that covers an octave spectrum. For Ti:sapphire laser, the spectrum extends from 500 to 1000 nm. When a narrow spectral pulse at 1000 nm light is frequency doubled, the interference between the second-harmonic pulse and the laser around 500 nm from the white-light leads to oscillation in the measured spectrum:

$$I(\omega) = I_{SH}(\omega) + I_{500}(\omega) + 2\sqrt{I_{SH}(\omega)I_{500}(\omega)}\cos(\omega\tau_d + \varphi_{CE}), \tag{7}$$

where $I_{SH}(\omega)$ and $I_{500}(\omega)$ are the power spectra of the second-harmonic and 500 nm pulses. τ_d is the delay between them. φ_{CE} is the CE phase of the laser pulses from the amplifier, which is also the CE phase for the 500 nm and 1000 nm pulses. When the CE phase is stabilized, the interference fringe does not shift with time, as shown in Fig. 4(a), where a 6 mJ, 30 fs operates at 1 kHz was

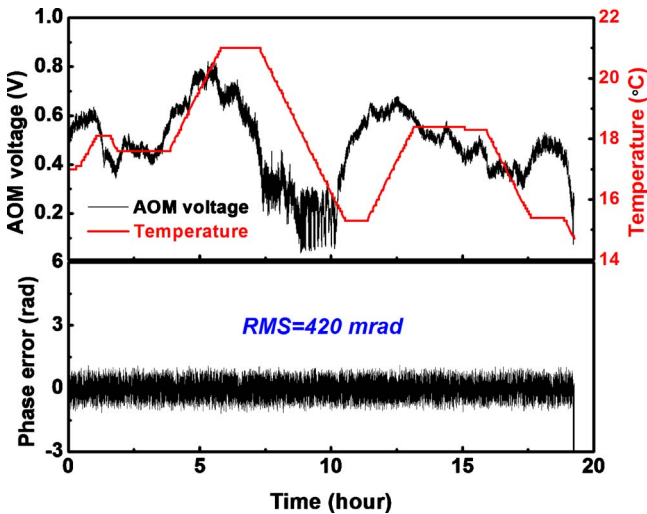


Fig. 3. (Color online) Locking the CE offset frequency by feedback-controlling the pump power and the crystal temperature. Reprinted from C. Yun, S. Chen, H. Wang, M. Chini, and Z. Chang, Appl. Opt. 48, 5127 (2009).

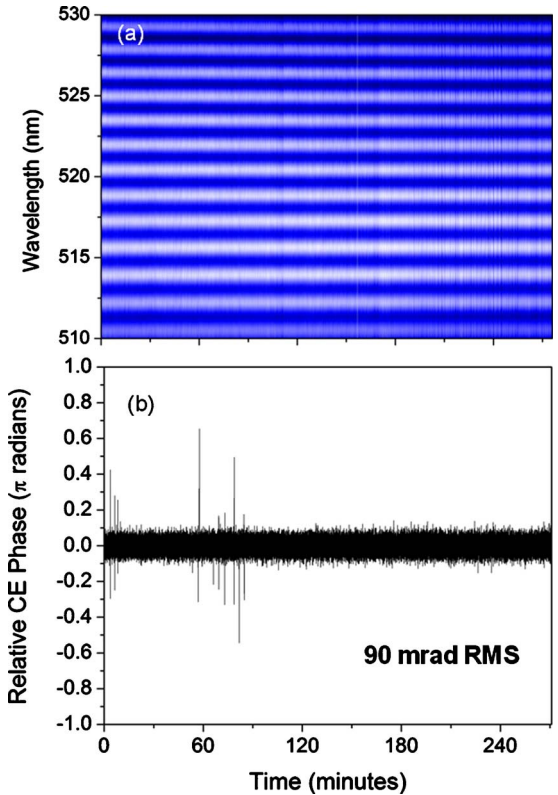


Fig. 4. (Color online) Stabilization of the CE phase a grating-based CPA. Reprinted from S. Chen, M. Chini, H. Wang, C. Yun, H. Mashiko, Y. Wu, and Z. Chang, Appl. Opt. 48, 5692 (2009).

locked to 90 mrad for 4.5 hours.

It was found that the systematic error of the measured CE phase is affected by the stability of the laser pulse energy. As large as 160 mrad of error can be introduced by a 1% laser energy fluctuation [34,35]. Techniques for locking the laser power have been developed to reduce the CE phase measurement error [36]. The CE phase of few-cycle pulses can be accurately measured with phase meters based on the above threshold ionization [37,38].

3. Automatic Phase Stabilization

The mid-IR laser pulses for generating attosecond pulses at shorter wavelengths can be produced with optical parametric amplifiers (OPAs). In an OPA, a nonlinear crystal is pumped by the femtosecond pulse from a CPA laser. The signal pulse that seeds the OPA can be generated by focusing a small portion of the CPA pulse into a sapphire plate, like in the case of white-light generation in f -to- $2f$ interferometers. We can assume that the CE phase of the signal, $\varphi_{CE,s}$, and the pump pulses, $\varphi_{CE,p}$, are the same since they are from the same CPA laser. The CE phase of the idler pulse

$$\varphi_{CE,i} = \varphi_{CE,p} - \varphi_{CE,s} \tag{8}$$

is constant. Thus the CE phase of the idler pulse is automatically stabilized even if the CE phase of the CPA laser changes from shot to shot [39–41].

4. ISOLATED ATTOSECOND LIGHT SOURCE

Both the semiclassical model and the strong field model predicted that attosecond pulse trains are produced when

the driving laser is linearly polarized and contains many optical cycles of oscillation. The spacing between the neighboring pulses is half of laser optical cycle, which is 1.3 fs for Ti:sapphire lasers. Once the pulse train is generated, it is extremely difficult to switch out a single isolated pulse from the train. For that to work, one would need a pulse picker that opens for less than an optical cycle.

Single isolated attosecond pulses have been directly generated from gas targets since 2001. Several sub-cycle gating methods have been developed that can be applied to the generation stage.

A. Amplitude Gating

If the driving laser is a half-cycle pulse, the three-step process can only occur once, which naturally generates a single attosecond pulse. Half-cycle picosecond pulses in the THz frequency range have been extensively used in studying Rydberg atoms [42]. However, the generation of high-power half-cycle pulses in the visible to mid-IR range is extremely challenging. The shortest sub-millijoule laser near 800 nm that has been measured so far is 3.8 fs [43], which is still longer than one optical period (2.5 fs). Consequently, at least two attosecond pulses are generated. The number of XUV pulses can be reduced to one by spectrally filtering out the cut-off region of the XUV spectrum and by stabilizing the CE phase of the driving laser [44]. The first experimental demonstration of isolated attosecond pulse generation in 2001 was performed with a 7 fs laser [45]. The 650 as pulse duration was deduced from the attosecond streak camera trace. The shortest XUV pulse, 80 as, was generated in 2008 by using CE phase stabilized 3.8 fs lasers [43].

B. Polarization Gating

The amplitude gating only makes use of the cut-off region of the XUV spectrum, the narrow spectrum range put a limit on the attosecond pulse duration. Dumping the broad plateau spectrum also reduces the conversion efficiency from the NIR driving laser to the XUV pulses. Polarization gating is an alternative sub-cycle gating method that can generate isolated attosecond pulse in both the plateau and cut-off region of the XUV spectrum.

Attosecond pulses can only be efficiently generated with linearly polarized driving field, which can be easily understood by using the three-step model. If the laser is elliptically or circularly polarized, the returning electrons are steered away from the parent ion, which reduces the recombination probability. When the ellipticity reaches 0.2, the attosecond generation yield drops by about an order of magnitude. If the driving field is such that only a small portion under its envelope is linearly polarized, whereas the other portions are circularly polarized, then a single XUV pulse can be generated as long as the linear portion is short enough [46].

The driving pulse for polarization gating can be constructed by the superposition of two counter-rotating circularly or elliptically polarized pulses with a certain delay T_d between them [47–50]. For such pulses, the width of the polarization gate can be estimated by the expression [49–51]

$$\delta t_G \approx \frac{\xi_{th}(\eta, q) \epsilon \tau_p^2}{\ln(2) T_d}, \quad (9)$$

where $\xi_{th} \approx 0.2$ is the threshold ellipticity at which the q^{th} harmonic intensity drops to a certain value, $\eta \approx 0.1$, of that generated by linearly polarized lasers. τ_p is the duration of each elliptically polarized pulse with an ellipticity ϵ .

Equation (9) indicates that it is possible to reduce the gate width to sub-laser cycle by properly choosing three laser parameters, ϵ , τ_p , and T_d . However, the attosecond yield decreases with the laser pulse length due to the depletion of the ground-state population of the target atoms [49]. Numerical simulations showed that, by using 5 fs driving lasers, it is possible to generate sub-100 as pulses in the plateau region of the XUV spectrum when the positive chirp of the attosecond pulse is compensated by negative dispersions of thin films [52].

Experimentally, the effects of the polarization gating on the sub-laser cycle was demonstrated by the generation of XUV supercontinuum [53]. The sub-10 fs driving laser pulses were generated in a hollow-core fiber pulse compressor. XUV pulses as short as 130 as were generated with 5 fs CE phase stabilized NIR lasers [54]. In these experiments, the laser pulses with a time-dependent ellipticity were created by using birefringence optics. Higher-energy driving pulses for polarization gating could be produced by using interferometers [55].

C. Double Optical Gating

When a second-harmonic field is added to the fundamental driving laser field, the spacing between the neighboring attosecond pulses become a full laser cycle, due to the symmetry breaking of the driving field. This process is named two-color gating [56]. The combination of the polarization gating with two-color gating leads to a new sub-cycle gating method: double optical gating. Due to the increased pulse spacing, the required polarization gate width can be set wider, which allows longer driving lasers to be used for generating isolated attosecond pulses [57,58]. The experimental setup that demonstrated the generation of isolated 163 as pulse using 25 fs Ti:sapphire laser is depicted in Fig. 5. The linearly polarized 2 mJ pulses centered at 780 nm from a chirped pulse amplifier operating at 1.5 kHz were transformed into the gating field with a time-dependent ellipticity through four optical elements, as shown in Fig. 5(a), which include a second-harmonic generation crystal BBO. They are placed in one arm of the attosecond streak camera shown in Fig. 5(b) to generate the XUV pulses. The measured CRAB trace and the reconstructed attosecond pulse are shown in Fig. 6 [51,59].

The capability of the generating isolated pulses using 25 fs lasers has several advantages. First, the photon flux can be scaled up by many orders of magnitude with ~ 100 TW lasers. This is important for studying nonlinear processes with isolated attosecond pulses. Second, such lasers are easier to construct and operate. This allows many labs where 25 fs CPA systems are already available to conduct attosecond research. Finally, like polarization gating, a double optical gating can produce isolated at-

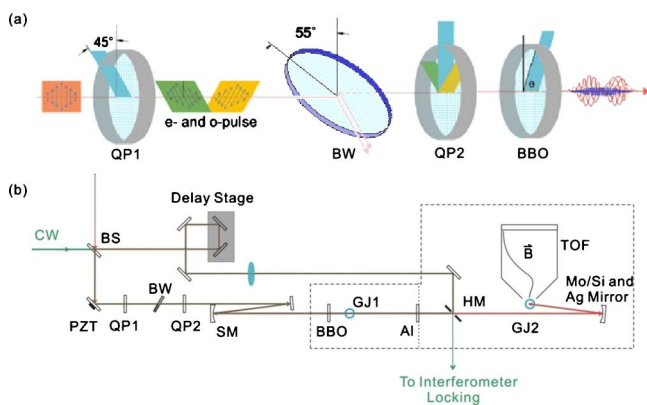


Fig. 5. (Color online) Experimental setup for implementing double optical gating to generate isolated attosecond pulses with 25 fs lasers directly from CPA amplifiers. Reprinted from S. Gilbertson, Y. Wu, S. D. Khan, M. Chini, K. Zhao, X. Feng, and Z. Chang, *Phys. Rev. A* **81**, 043810 (2010).

tosecond pulses in both the cut-off and plateau region. A soft X-ray supercontinuum extending over 600 eV has been generated, which is ideal for transient absorption applications [60].

5. OUTLOOK

We have introduced the core technologies that are essential to attosecond pulse generation. These technologies are now relatively mature. However, as we refine attosecond technology over the next decade, we should expect pulse durations to fall a lot more. We will find better methods to correct chirp. We will develop better schemes for attosecond gating. We will use other driving fields, extending the spectrum and bandwidth toward ~ 1000 eV. It seems inevitable that pulse durations will fall by another order of magnitude or more, easily passing one atomic unit.

However, it is not necessary to develop perfect chirp compensation for all high time-resolution experiments. A chirped pulse can be used as if it were transformed limited as long as the chirp is known [61].

But it is not only the pulse duration that makes high harmonic generation so important. High harmonics cover a spectral region in which coherent light is unavailable. Thus, high harmonics is a unique source that can compete with synchrotrons for some VUV and perhaps XUV experiments—it may even compete with X-ray free electron lasers in these wavelength regions.

But it is not only the frequency and pulse duration that drive applications. Just as perturbative nonlinear optics has many applications other than those in ultrafast science, so too nonperturbative nonlinear optics will find applications other than those directly related to attosecond dynamics. Nonperturbative nonlinear optics offers a completely new approach to some problems. Tunneling, for example, is one of the most important quantum mechanical phenomena. It is almost inconceivable that, having tunneling at the core of most of our experiments, we cannot exploit it. Imagine an electron tunneling from a molecule. The molecule serves the function of a tunneling tip. Rotating the molecule is much like scanning the tip. Measuring the ionization probability as a function of time we can trace out a molecular orbital structure [10,11,62].

The re-collision electron also has greater implications than just forming attosecond pulses to be used elsewhere. It can be thought of as an attosecond electron beam aimed right at the molecule from which it tunneled [8]. With a wavelength in the $0.5 \text{ \AA} < \lambda < 3 \text{ \AA}$, the electron can serve as an extremely interesting probe of atomic scale matter. An electron with this wavelength will diffract. Measuring the electron, we measure the atomic-scale structure of the ion [7,10,63]. The electron can also interfere with the electron from which it departed—this interference is the source of high harmonic generation [9]. Thus the har-

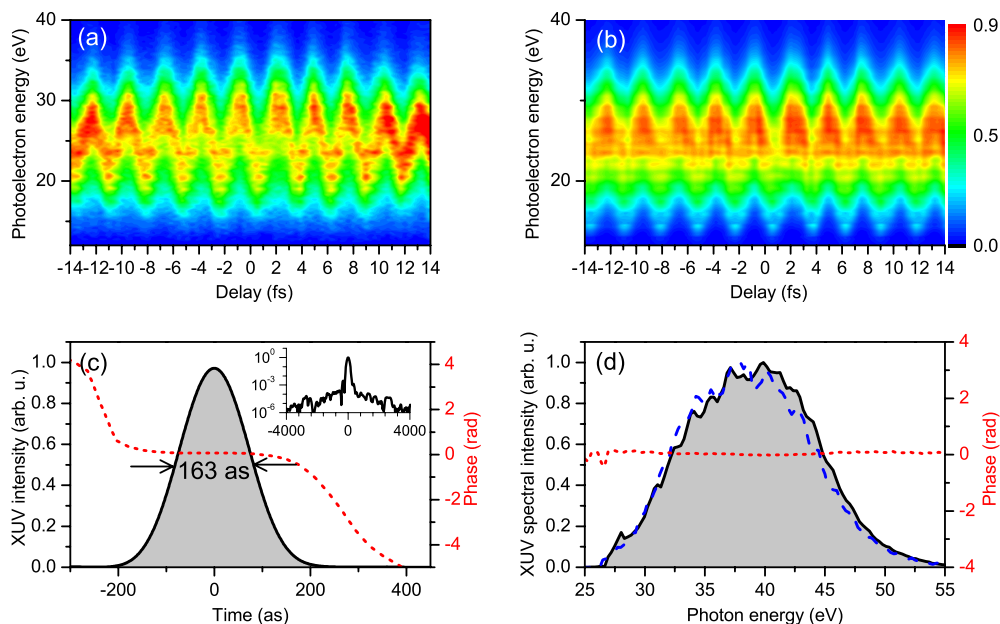


Fig. 6. (Color online) Characterization of the isolated attosecond pulses generated with 25 fs lasers with CRAB. Reprinted from S. Gilbertson, Y. Wu, S. D. Khan, M. Chini, K. Zhao, X. Feng, and Z. Chang, *Phys. Rev. A* **81**, 043810 (2010).

monic spectrum encodes the orbital structure of matter [9] just as optical interferometry measures the temporal or spatial structure of an optical beam.

Removing our optical bias and looking on a grander scale, re-collision science is a unique mixture of optical and collision physics. As we have just seen, optics can borrow from collision physics the ability to image atomic-scale matter. Equally, collision physics can transfer from optics the ability to perform time-resolved experiments [63,64]. This may extend even up to measuring dynamics in the atomic nucleus [65,66].

As we approach the second attosecond decade, it is clear that there are new frontiers opening everywhere. Already attosecond science is influencing fields other than our own—but then this is not an unusual trajectory for a new optical technology.

ACKNOWLEDGMENTS

The authors jointly acknowledge support by the United States Army Research Office (USARO) under grant W911NF-07-1-0475. ZC acknowledges the United States Department of Energy (DOE) for funding his research.

REFERENCES

- P. B. Corkum, "Plasma perspective on strong-field multiphoton ionization," *Phys. Rev. Lett.* **71**, 1994–1997 (1993).
- E. Constant, V. Taranukhin, A. Stolow, and P. B. Corkum, "Methods for the measurement of the duration of high-harmonic pulses," *Phys. Rev.* **A56**, 3870–3878 (1997).
- A. L. Cavalieri, N. Müller, Th. Uphues, V. S. Yakovlev, A. Baltuška, B. Horvath, B. Schmidt, L. Blümel, R. Holzwarth, S. Hendel, M. Drescher, U. Kleineberg, P. M. Echenique, R. Kienberger, F. Krausz, and U. Heinzmann, "Attosecond spectroscopy in condensed matter," *Nature* **449**, 1029–1032 (2007).
- H. Wörner, J. Bertrand, D. Kartashov, P. B. Corkum, and D. M. Villeneuve, "Attosecond homodyne interferometry of a chemical reaction," *Nature* **466**, 604–607 (2010).
- A. Staudte, D. Pavicic, D. Zeidler, M. Meckel, H. Niikura, M. Schoffler, S. Schosler, B. Ulrich, P. P. Rajeev, Th. Weber, T. Jahnke, D. M. Villeneuve, S. Chelkowski, A. D. Bandrauk, C. L. Cocke, P. B. Corkum, and R. Dörner, "Attosecond strobing of 2-surface population dynamics in dissociating H_2^+ ," *Phys. Rev. Lett.* **98**, 073003 (2007).
- H. Niikura, F. Légaré, R. Hasbani, M. Yu. Ivanov, D. M. Villeneuve, and P. B. Corkum, "Using correlated pairs for sub-femtosecond-resolution wave packet measurements," *Nature* **421**, 826–829 (2003).
- T. Zuo, A. D. Bandrauk, and P. B. Corkum, "Laser induced electron diffraction: a new tool for probing ultrafast molecular dynamics," *Chem. Phys. Lett.* **259**, 313–320 (1996).
- H. Niikura, F. Légaré, R. Hasbani, A. D. Bandrauk, M. Yu. Ivanov, D. M. Villeneuve, and P. B. Corkum, "Sub-laser-cycle electron pulses for probing molecular dynamics," *Nature* **417**, 917–922 (2002).
- J. Itatani, J. Levesque, D. Zeidler, H. Niikura, H. Pepin, J. C. Kieffer, P. B. Corkum, and D. M. Villeneuve, "Tomographic imaging of molecular orbitals," *Nature* **432**, 867–871 (2004).
- M. Meckel, D. Comtois, D. Zeidler, A. Staudte, H. C. Bandulet, D. Pavicic, H. Pepin, J. C. Kieffer, R. Dörner, D. M. Villeneuve, and P. B. Corkum, "Laser induced electron tunneling and diffraction," *Science* **320**, 1478–1482 (2008).
- H. Akagi, T. Otobe, A. Staudte, A. Shiner, F. Turner, R. Dörner, D. M. Villeneuve, and P. B. Corkum, "Direct observation of tunneling from HOMO-1 in HCl," *Science* **325**, 1364–1367 (2009).
- M. Lein, "Molecular imaging using re-collision electrons," *J. Phys. B* **40**, R135–R173 (2007).
- K. C. Kulander, K. J. Schafer, and J. L. Krause, "Dynamics of short-pulse excitation, ionization and harmonic conversion," in *Super-Intense Laser-Atom Physics, NATO ASI, Ser. B*, Vol. 316 (Plenum, 1993), pp. 95–110.
- M. V. Ammosov, N. B. Delone, and V. P. Krainov, "Tunnel ionization of complex atoms and atomic ions in an alternating electromagnetic field," *Sov. Phys. JETP* **64**, 1191–1194 (1986).
- Z. Chang, A. Rundquist, H. Wang, H. Kapteyn, and M. Murnane, "Generation of coherent soft X-rays at 2.7 nm using high harmonics," *Phys. Rev. Lett.* **79**, 2967–2970 (1997).
- B. Shan and Z. Chang, "Dramatic extension of the high-order harmonic cut-off by using a long-wavelength pump," *Phys. Rev. A* **65**, 011804(R) (2001).
- E. J. Takahashi, T. Kanai, K. L. Ishikawa, Y. Nabekawa, and K. Midorikawa, "Coherent water window X ray by phase-matched high-order harmonic generation in neutral media," *Phys. Rev. Lett.* **101**, 253901 (2008).
- T. Popmintchev, M.-C. Chen, O. Cohen, M. E. Grisham, J. J. Rocca, M. M. Murnane, and H. C. Kapteyn, "Extended phase matching of high harmonics driven by mid-infrared light," *Opt. Lett.* **33**, 2128–2130 (2008).
- H. Xiong, H. Xu, Y. Fu, J. Yao, B. Zeng, W. Chu, Y. Cheng, Z. Xu, E. J. Takahashi, K. Midorikawa, X. Liu, and J. Chen, "Generation of a coherent x ray in the water window region at 1 kHz repetition rate using a mid-infrared pump source," *Opt. Lett.* **34**, 1747–1749 (2009).
- M. Lewenstein, P. Balcou, M. Ivanov, A. L'Huillier, and P. B. Corkum, "Theory of high-harmonic generation by low frequency laser fields," *Phys. Rev. A* **49**, 2117–2132 (1994).
- J. Itatani, F. Quéré, G. L. Yudin, M. Yu. Ivanov, F. Krausz, and P. B. Corkum, "Attosecond streak camera," *Phys. Rev. Lett.* **88**, 173903 (2002).
- M. Kitzler, N. Milosevic, A. Scrinzi, F. Krausz, and T. Bräbäck, "Quantum theory of attosecond XUV pulse measurement by laser dressed photoionization," *Phys. Rev. Lett.* **88**, 173904 (2002).
- R. Trebino and D. J. Kane, "Using phase retrieval to measure the intensity and phase of ultrashort pulses: frequency-resolved optical gating," *J. Opt. Soc. Am. A* **10**, 1101–1111 (1993).
- Y. Mairesse and F. Quéré, "Frequency-resolved optical gating for complete reconstruction of attosecond bursts," *Phys. Rev. A* **71**, 011401(R) (2005).
- M. Chini, S. Gilbertson, S. D. Khan, and Z. Chang, "Characterizing ultrabroadband attosecond lasers," *Opt. Express* **18**, 13006–13016 (2010).
- Z. Chang, "Carrier envelope phase shift caused by grating-based stretchers and compressors," *Appl. Opt.* **45**, 8350–8353 (2006).
- A. Apolonski, A. Poppe, G. Tempea, Ch. Spielmann, Th. Udem, R. Holtzwarth, T. W. Hänsch, and F. Krausz, "Controlling the phase evolution of few-cycle light pulses," *Phys. Rev. Lett.* **85**, 740–743 (2000).
- D. J. Jones, S. A. Diddams, J. K. Ranka, A. Stentz, R. S. Windeler, J. L. Hall, and S. T. Cundiff, "Carrier-envelope phase control of femtosecond mode-locked lasers and direct optical frequency synthesis," *Science* **288**, 635–640 (2000).
- C. Yun, S. Chen, H. Wang, M. Chini, and Z. Chang, "Temperature feedback control for long-term carrier-envelope phase locking," *Appl. Opt.* **48**, 5127–5130 (2009).
- C. Li, E. Moon, H. Mashiko, C. Nakamura, P. Ranitovic, C. L. Cocke, and Z. Chang, G. G. Paulus, "Precision control of carrier-envelope phase in grating based chirped pulse amplifiers," *Opt. Express* **14**, 11468–11476 (2006).
- S. Chen, M. Chini, H. Wang, C. Yun, H. Mashiko, Y. Wu, and Z. Chang, "Carrier-envelope phase stabilization and control of 1 kHz, 6 mJ, 30 fs laser pulses from a Ti:sapphire regenerative amplifier," *Appl. Opt.* **48**, 5692–5695 (2009).
- M. Kakehata, H. Takada, Y. Kobayashi, K. Torizuka, Y.

- Fujihira, T. Homma, and H. Takahashi, "Single-shot measurement of carrier-envelope phase changes by spectral interferometry," *Opt. Lett.* **26**, 1436–1438 (2001).
33. A. Baltuška, M. Uiberacker, E. Goulielmakis, R. Kienberger, V. S. Yakovlev, T. Udem, T. W. Hänsch, and F. Krausz, "Phase controlled amplification of few-cycle laser pulses," *IEEE J. Quantum Electron.* **9**, 972–989 (2003).
 34. C. Li, E. Moon, H. Wang, H. Mashiko, C. M. Nakamura, J. Tackett, and Z. Chang, "Determining the phase-energy coupling coefficient in carrier-envelope phase measurements," *Opt. Lett.* **32**, 796–798 (2007).
 35. C. Li, E. Moon, H. Mashiko, H. Wang, C. M. Nakamura, J. Tackett, and Z. Chang, "Mechanism of phase-energy coupling in *f*-to-*2f* interferometry," *Appl. Opt.* **48**, 1303–1307 (2009).
 36. H. Wang, C. Li, J. Tackett, H. Mashiko, C. M. Nakamura, E. Moon, and Z. Chang, "Power locking of high-repetition-rate chirped pulse amplifiers," *Appl. Phys. B* **89**, 275–279 (2007).
 37. P. Dietrich, F. Krausz, and P. B. Corkum, "Determining the absolute carrier phase of a few cycle pulses," *Opt. Lett.* **25**, 16–18 (2000).
 38. G. G. Paulus, F. Lindner, H. Walther, A. Baltuška, E. Goulielmakis, M. Lezius, and F. Krausz, "Measurement of the phase of few-cycle laser pulses," *Phys. Rev. Lett.* **91**, 253004 (2003).
 39. A. Baltuska, T. Fuji, and T. Kobayashi, "Controlling the carrier envelope phase of ultrashort light pulses with optical parametric amplifiers," *Phys. Rev. Lett.* **88**, 133901 (2002).
 40. C. Vozzi, F. Calegari, E. Benedetti, S. Gasilov, G. Sansone, G. Cerullo, M. Nisoli, S. De Silvestri, and S. Stagira, "Millijoule-level phase-stabilized few-optical-cycle infrared parametric source," *Opt. Lett.* **32**, 2957–2959 (2007).
 41. C. Vozzi, F. Calegari, F. Frassetto, M. Negro, L. Poletto, G. Sansone, P. Villoresi, M. Nisoli, S. Silvestri, and S. Stagira, "High order harmonics driven by a self-phase-stabilized IR parametric source," *Laser Phys.* **5**, 1019–1027 (2010).
 42. R. R. Jones, D. You, and P. H. Bucksbaum, "Ionization of Rydberg atoms by subpicosecond half-cycle electromagnetic pulses," *Phys. Rev. Lett.* **70**, 1236–1239 (1993).
 43. E. Goulielmakis, M. Schultze, M. Hofstetter, V. S. Yakovlev, J. Gagnon, M. Uiberacker, A. L. Aquila, E. M. Gullikson, D. T. Attwood, R. Kienberger, F. Krausz, and U. Kleineberg, "Single-cycle nonlinear optics," *Science* **320**, 1614–1617 (2008).
 44. I. P. Christov, M. M. Murnane, and H. C. Kapteyn, "High-harmonic generation of attosecond pulses in the "single-cycle" regime," *Phys. Rev. Lett.* **78**, 1251–1254 (1997).
 45. M. Hentschel, R. Kienberger, Ch. Spielmann, G. A. Reider, N. Milosevic, T. Brabec, P. Corkum, U. Heinzmann, M. Drescher, and F. Krausz, "Attosecond metrology," *Nature* **414**, 509–513 (2001).
 46. P. B. Corkum, N. H. Burnett, and M. Y. Ivanov, "Subfemtosecond pulses," *Opt. Lett.* **19**, 1870–1872 (1994).
 47. V. T. Platonenko and V. V. Strelkov, "Single attosecond soft-x-ray pulse generated with a limited laser beam," *J. Opt. Soc. Am. B* **16**, 435–440 (1999).
 48. Dan Oron, Y. Silberberg, N. Dudovich, and D. M. Villeneuve, "Efficient polarization gating of high-order harmonic generation by polarization-shaped ultrashort pulses," *Phys. Rev. A* **72**, 063816 (2006).
 49. Z. Chang, "Single attosecond pulse and XUV supercontinuum in the high-order harmonic plateau," *Phys. Rev. A* **70**, 043802 (2004).
 50. V. Strelkov, A. Zair, O. Tcherbakoff, R. López-Martens, E. Cormier, E. Mével and E. Constant, "Single attosecond pulse production with an ellipticity-modulated driving IR pulse," *J. Phys. B* **38**, L161–L167 (2005).
 51. X. Feng, S. Gilbertson, H. Mashiko, H. Wang, S. D. Khan, M. Chini, Y. Wu, K. Zhao, and Z. Chang, "Generation of isolated attosecond pulses with 20 to 28 femtosecond lasers," *Phys. Rev. Lett.* **103**, 183901 (2009).
 52. Z. Chang, "Chirp of the attosecond pulses generated by a polarization gating," *Phys. Rev. A* **71**, 023813 (2005).
 53. B. Shan, S. Ghimire, and Z. Chang, "Generation of attosecond XUV supercontinuum by polarization gating," *J. Mod. Opt.* **52**, 277–283 (2005).
 54. G. Sansone, E. Benedetti, F. Calegari, C. Vozzi, L. Avaldi, Flammini, L. Poletto, P. Villoresi, C. Altucci, R. Velotta, S. Stagira, S. De Silvestri, and M. Nisoli, "Isolated single-cycle attosecond pulses," *Science* **314**, 443–446 (2006).
 55. P. Tzallas, E. Skantzakis, C. Kalpouzos, E. P. Benis, G. D. Tsakiris, and D. Charalambidis, "Generation of intense continuum extreme-ultraviolet radiation by many-cycle laser fields," *Nat. Phys.* **3**, 846–850 (2007).
 56. J. Mauritsson, P. Johnsson, E. Gustafsson, A. L'Huillier, K. J. Schafer, and M. B. Gaarde, "Attosecond pulse trains generated using two color laser fields," *Phys. Rev. Lett.* **97**, 013001 (2006).
 57. Z. Chang, "Controlling attosecond pulse generation with a double optical gating," *Phys. Rev. A* **76**, 051403(R) (2007).
 58. H. Mashiko, S. Gilbertson, C. Li, S. D. Khan, M. M. Shakya, E. Moon, and Z. Chang, "Double optical gating of high-order harmonic generation with carrier-envelope phase stabilized lasers," *Appl. Phys. Lett.* **100**, 103906 (2008).
 59. S. Gilbertson, Y. Wu, S. D. Khan, M. Chini, K. Zhao, X. Feng, and Z. Chang, "Isolated attosecond pulse generation using multicycle pulses directly from a laser amplifier," *Phys. Rev. A* **81**, 043810 (2010).
 60. H. Mashiko, S. Gilbertson, X. Feng, C. Yun, S. D. Khan, H. Wang, M. Chini, C. Shouyuan, and Z. Chang, "XUV supercontinua supporting pulse durations of less than one atomic unit of time," *Opt. Lett.* **34**, 3337–3339 (2009).
 61. G. L. Yudin, A. D. Bandrauk, and P. B. Corkum, "Chirped attosecond photoelectron spectroscopy," *Phys. Rev. Lett.* **96**, 063002 (2006).
 62. A. Staudte, S. Patchkovskii, D. Pavicic, H. Akagi, O. Smirnova, D. Zeidler, M. Meckel, D. M. Villeneuve, R. Dörner, M. Ivanov, and P. B. Corkum, "Angular tunneling ionization probability of H₂," *Phys. Rev. Lett.* **102**, 033004 (2009).
 63. M. Okunishi, T. Morishita, G. Prumper, K. Shimada, C. D. Lin, S. Watanabe, and K. Ueda, "Experimental retrieval of target structure information from laser-induced rescattered photoelectron momentum distributions," *Phys. Rev. Lett.* **100**, 143001 (2008).
 64. A. Emmanouilidou, A. Staudte, and P. B. Corkum, "Time-resolving inter-atomic two-electron collision dynamics," *ArXiv:1003.1593v1* (2010).
 65. N. Milosevic, P. B. Corkum, and T. Brabec, "How to use lasers for imaging attosecond dynamics of nuclear processes," *Phys. Rev. Lett.* **92**, 013002 (2004).
 66. S. Chelkowski, A. D. Bandrauk, and P. B. Corkum, "Control of nuclear processes with super-intense laser pulses," *Phys. Rev. Lett.* **93**, 083602 (2004).